

5.9 Strangulation of the baroclinic flow by the barotropic flow.

Our treatment of the rotating, two-layer hydraulics is concluded with a discussion of the case in which the channel is dynamically wide, at least on the scale of the global internal Rossby radius of deformation. This limit is quite the opposite of what is assumed in the theory of zero potential vorticity flow. As we shall see, the internal, or ‘baroclinic’, dynamics occur within right- and left-wall boundary layers that are physically separated from each other. Although the theory for this flow has not been widely applied, it is useful in illustrating a physical process that was either lacking or hidden on our previous discussions. This process is the forcing of the baroclinic boundary layers by the barotropic (depth independent) part of the flow. Unlike the former, the latter extends all the way across the channel and is altered by changes in the channel width or depth. The baroclinic flow is forced directly through interactions with the barotropic flow, leading to some novel and unexpected behavior. For one thing, a new type of hydraulic control emerges. The following treatment is based on a model developed by Pratt and Armi (1990) and having uniform potential vorticity in each layer.

Consider a channel with varying width but constant bottom elevation ($h^*=0$), so that z_T^* is the total depth (Figure 5.9.1a). The potential vorticity is uniform in each of the two layers, the corresponding potential depths are $D_{1\infty}$ and $D_{2\infty}$, and the internal Rossby radius of deformation L_I is given by (5.1.12). We will only treat flows for which the layer depths are finite all across the channel, so that the interface contacts the two sidewalls and not the top or bottom. Solving (5.1.11) for the lower layer depth d_2^* , and using the rigid lid constraint $d_1^* = z_T^* - d_2^*$ yield the following depth profiles

$$d_1(x, y, t) = - \left[\frac{(\eta_+(y, t) + \eta_-(y, t)) \cosh(x)}{2 \cosh(w(y)/2)} + \frac{(\eta_+(y, t) - \eta_-(y, t)) \sinh(x)}{2 \sinh(w(y)/2)} \right] + \Delta \quad (5.9.1)$$

$$d_2(x, y, t) = \left[\frac{(\eta_+(y, t) + \eta_-(y, t)) \cosh(x)}{2 \cosh(w(y)/2)} + \frac{(\eta_+(y, t) - \eta_-(y, t)) \sinh(x)}{2 \sinh(w(y)/2)} \right] + \Delta / \hat{\delta} \quad (5.9.2)$$

where $\Delta = D / (D_{1\infty} + D_{2\infty})$, $\hat{\delta} = D_{1\infty} / D_{2\infty}$ and where the nondimensional variables

$$d_n = d_n^* / D_{1\infty}, \quad v_n = v_n^* / fL_I, \quad \text{and} \quad (x, y) = (x^*, y^*) / L_I.$$

have been introduced. Also η_+ and η_- denote the deviations of the interface elevation at the right ($x=w/2$) and left ($y=-w/2$) walls, as shown in the figure. It is not difficult to show that the conditions that the interface remains attached to the sidewalls is

$$-\Delta / \hat{\delta} \leq \eta_{\pm} \leq \Delta.$$

very rough draft-not for distribution

The depth profiles have a boundary layer structure that is apparent when the channel width is much wider than the internal deformation radius ($w \gg 1$). In this limit the layer thicknesses in the interior of the channel, away from the boundary layers, become

$$d_1 = \Delta, \text{ or } d_1^* = z_T^* \frac{D_{1\infty}}{D_{1\infty} + D_{2\infty}}$$

and

$$d_2 = \Delta / \hat{\delta}, \text{ or } d_2^* = z_T^* \frac{D_{2\infty}}{D_{1\infty} + D_{2\infty}}.$$

Thus the ratio of an interior layer depth to the total depth is equal to the ratio of its potential depth to the sum of the potential depths. If the potential depths are equal then the interior layer thicknesses are also equal. Unless the sum of the potential depths happens to be equal the total depth, the interior layer thicknesses are not equal to their potential depths. The interior flow can therefore have horizontal vorticity even though the interface is level.

The last remark can be verified by examining the velocity profiles for the two layers:

$$v_1(x, y, t) = - \left[\frac{(\eta_+(y, t) + \eta_-(y, t)) \sinh(x)}{2 \cosh(w(y) / 2)} + \frac{(\eta_+(y, t) - \eta_-(y, t)) \cosh(x)}{2 \sinh(w(y) / 2)} \right] + (\Delta - 1)x + V(y, t) \quad (5.9.3)$$

and

$$v_2(x, y, t) = \hat{\delta} \left[\frac{(\eta_+(y, t) + \eta_-(y, t)) \sinh(x)}{2 \cosh(w(y) / 2)} + \frac{(\eta_+(y, t) - \eta_-(y, t)) \cosh(x)}{2 \sinh(w(y) / 2)} \right] + (\Delta - 1)x + V(y, t), \quad (5.9.4)$$

which can be obtained from the potential vorticity equations (5.1.9 and 5.1.10) with the known thickness profiles. Each velocity is composed of a baroclinic component (term in large brackets) having opposite sign in each layer, and a barotropic, or depth-independent component $(\Delta - 1)x + V(y, t)$. The latter consists of a part that has a constant vorticity $\Delta - 1$, but no cross-sectional mean, and a part that is x -independent.¹ It is clearly the first of these that accounts for the presence of vorticity in the interior. Only when the sum of the potential depths is equal to the channel depth ($\Delta=1$) does this vorticity vanish. In this case the interior layer thicknesses equal their potential depths. The physical mechanism responsible for the presence of barotropic shear can be described by imagining that the channel is fed from a reservoir where the fluid is at rest and where the layer depths are

¹ If the fluid had a free surface and thus an external deformation radius, the shear would be confined to boundary layers having that width, as in the Gill (1977) model. The surface on our channel is rigid, which is equivalent to having an infinite external deformation radius. The result is that the barotropic shear is uniform.

very rough draft-not for distribution

therefore equal to $D_{1\infty}$ and $D_{2\infty}$ throughout. If the total depth $D_{1\infty} + D_{2\infty}$ in the reservoir is different from the channel depth z_T^* , then the water column as a whole undergoes squashing or stretching upon entering the channel. The result is that barotropic vorticity is spun up or down. Note that the lock exchange calculation of the previous section had $\Delta=1$ and $V=0$, so that the barotropic component of velocity was zero.

The total volume flux is given by

$$Q = \int_{-w/2}^{w/2} (v_1 d_1 + v_2 d_2) dx = \frac{1}{2}(1 + \hat{\delta})(\eta_+^2 - \eta_-^2) + z_T w V, \quad (5.9.5)$$

where $z_T = z_T^* / D_{1\infty} = \Delta(1 + \hat{\delta}) / \hat{\delta}$. The two terms on the right-hand side measure the contributions from the baroclinic and barotropic parts of the flow.

We now restrict attention to a channel that is very wide compared to L_I , or $w \gg 1$. The baroclinic boundary layers are then well separated and the layer velocities at the sidewalls reduce to

$$v_1(\pm \frac{1}{2} w(y), y, t) = \mp \eta_{\pm} \pm \frac{1}{2}(\Delta - 1)w + V \quad (5.9.6)$$

and

$$v_2(\pm \frac{1}{2} w(y), y, t) = \pm \tilde{\delta} \eta_{\pm} \pm \frac{1}{2}(\Delta - 1)w + V. \quad (5.9.7)$$

The dimensional characteristic speeds of the internal Kelvin waves that propagate along the walls at $\pm w/2$ are given by

$$c_{\pm}^* = \frac{v_1^*(\pm \frac{1}{2} w^*(y^*), x^*, t^*) D_{2\infty} + v_2^*(\pm \frac{1}{2} w^*(y^*), x^*, t^*) D_{1\infty}}{D_{1\infty} + D_{2\infty}} \pm \left(\frac{g' D_{1\infty} D_{2\infty}}{D_{1\infty} + D_{2\infty}} \right)^{1/2} \quad (5.9.8)$$

(see Exercise 2.) The dimensionless equivalent $c_{\pm} = c_{\pm}^* / (g' D_{1\infty})^{1/2}$ is given by

$$c_{\pm} = \frac{\mp(1 - \hat{\delta})\eta_{\pm} \pm \frac{1}{2}(\Delta - 1)w + V \pm 1}{(1 + \hat{\delta})^{1/2}} \quad (5.9.9)$$

We now restrict attention to steady flow, for which the total volume transport Q is constant and the internal Bernoulli function ΔB^* is conserved along the sidewalls. In the limit $w \gg 1$, Q as given by (5.9.5) is dominated by the contribution from the barotropic velocity V , which is uniformly distributed across the channel. Thus

$$Q = V w z_T \quad (5.9.10)$$

in this limit. Also the dimensionless internal Bernoulli function $\Delta B^* / (g' D_{1\infty})^{1/2}$ on the left and right side walls (see 5.1.17) are given by

$$\Delta B_{\pm} = \frac{1}{2}(\hat{\delta} - 1)\eta_{\pm}^2 + [\frac{1}{2}(\Delta - 1)w \pm V + 1]\eta_{\pm} + \Delta / \hat{\delta}$$

where, again, '+' or '-' denote evaluation at $x=w/2$ or $x=-w/2$.² Elimination of V between these last two equations and rearrangement of the result leads to the functional relation

$$\mathcal{G}_{\pm}(\eta_{\pm}; w) = \eta_{\pm}^2 + s_{\pm}\eta_{\pm} + \mu_{\pm} = 0 \quad (5.9.11)$$

where

$$\mu_{\pm} = \frac{2}{\hat{\delta} - 1} \left(\frac{\Delta}{\hat{\delta}} - \Delta B_{\pm} \right)$$

and

$$s_{\pm} = \frac{2}{\hat{\delta} - 1} \left[\frac{1}{2}(\Delta - 1)w \pm \frac{Q}{wz_T} + 1 \right]. \quad (5.9.12)$$

Hence there are two hydraulic functions \mathcal{G}_+ and \mathcal{G}_- governing the independent baroclinic boundary currents along the right and left walls.

Happily, the hydraulic functions are quadratic in the dependent variables (either η_+ or η_-), and therefore simpler than the higher order or transcendental dependence we have encountered in earlier problems. The geometrical forcing is contained entirely in the coefficients $s_{\pm}(y)$, which depends on $w(y)$ in two ways. The first dependence involves the term $(\Delta - 1)w/2$, which is the value of the barotropic shear velocity $(\Delta - 1)x$ at the right wall. The second involves Q/wz_T , which is the value of the x -independent barotropic velocity. As w changes the boundary layer is displaced laterally across the barotropic shear and into regions where the barotropic shear velocity is higher or lower. At the same time, the mean barotropic velocity is increased or decreased by narrowing or widening of the channel. Both effects alter the total kinetic energy of the boundary flow, forcing the interface elevation and baroclinic velocity to adjust to maintain constant total energy. Because of the dual nature of this forcing mechanism, the maximum effective constriction of a particular boundary current need not occur at the point of minimum width. For this reason, we will refer to the parameter $s_{\pm}(y)$ as the *strangulation* in order to distinguish it from pure geometrical contraction. The most interesting solutions occur when both of the strangulation effects are in play and, since $w \gg 1$, this requires further parameter restrictions. Examination of (5.9.12) suggests that $\frac{1}{2}(\Delta - 1)w$ and Q/wz_T must balance, or

$$\Delta - 1 = O(Q/w^2). \quad (5.9.13)$$

² In equations with \pm subscripts the top or bottom '+' or '-' signs are used together. Thus $a_{\pm} = b_{\mp}$ means that $a_+ = b_-$ and $a_- = b_+$.

Thus the magnitude of the barotropic shear $\Delta - 1$ must be suitably small, preventing large shear velocities from forming at the sidewalls.

Conditions for critical flow can be found by taking $\partial \mathcal{G}_{\pm} / \partial \eta_{\pm} = 0$ leading to

$$\eta_{c_{\pm}} = -\frac{1}{2} s_{c_{\pm}} = -\frac{[\frac{1}{2}(\Delta - 1)w_c \pm (Q / w_c z_T) + 1]}{\hat{\delta} - 1}, \quad (5.9.14)$$

where the subscript ‘c’ denotes evaluation at a critical section. Comparison of the result with (5.9.9) verifies that $c_{\pm} = 0$. Note that the limit of equal potential depths ($\hat{\delta} \rightarrow 1$) must generally be avoided to avoid separation of the interface from one of the sidewalls.³

The compatibility condition that must hold at a critical section

$$\frac{\eta_{c_{\pm}}}{1 - \hat{\delta}} \left[\frac{1}{2}(\Delta - 1) \mp \frac{Q}{z_T w_c^2} \right] \left(\frac{dw}{dy} \right)_c = 0 \quad (5.9.15)$$

is obtained in the usual manner by taking $(d\mathcal{G}_{\pm}/dw)(dw/dy) = 0$. This relation suggests three distinct types of hydraulic controls. The first occurs at a point of extreme width $(dw / \partial y) = 0$ and is similar to the ‘narrows’ controls discussed in connection with single layer flows. The second occurs where η_{c+} or η_{c-} vanishes, depending on which boundary layer is being considered. If it is the left-hand boundary layer that is critical then (5.9.11) implies that $\Delta B_- = \Delta / \hat{\delta}$ and that the solution for all y is governed by the relation $\eta_-^2 + s_-(y)\eta_- = 0$. Solutions are given by $\eta_-(y) = 0$ and $\eta_- = -s_-(y)$. To interpret these solutions, note that the thermal wind relation (5.1.8) applied at the left wall can be written as

$$v_1(\pm w/2, y) - v_2(\pm w/2, y) = \pm(1 + \hat{\delta})\eta_{\pm} \quad (5.9.16)$$

The solution $\eta_-(y) = 0$ therefore has zero vertical shear for all y and shares some elements with the similarity solution discussed in Section 5.4 (and exemplified by the straight line energy curve with contour value .50 in Figure 5.4.1a). Note, however, that the nonrotating solution has $v_1^2 = v_2^2$ and is therefore shear free only for unidirectional flow. The solution $\eta_- = -s_-(y)$ has $\eta_- = 0$ only at the critical section but non-zero η .

³ If the fluid had a free surface and thus an external deformation radius of deformation, the shear would be confined to boundary layers having that width, as in the Gill (1977) model. However the lid on our channel is rigid, which is equivalent to having an infinite external deformation radius. The result is that the barotropic shear is uniform.

elsewhere⁴. Similar properties are possible for the boundary current on the right wall. In analogy with the nonrotating solutions we will call a control with $\eta_+ = 0$ or $\eta_- = 0$ a virtual control. As before, there are no restrictions on the value of w at such a control.

The third type of control occurs where the strangulation $s(y)$ reaches an extreme value away from an extreme value of w . We refer to this type of critical flow as a *remote* control and note that it requires vanishing of the bracketed term in (5.9.15) for either the '+' or '-' sign. Thus

$$w_c = \pm \left(\frac{2Q}{z_T(\Delta - 1)} \right)^{1/2} \quad (5.9.17)$$

for a remote control in a right-hand boundary layer, and

$$w_c = \pm \left(\frac{-2Q}{z_T(\Delta - 1)} \right)^{1/2} \quad (5.9.18)$$

for the left-hand boundary layer. For fixed values of Q and Δ only one of these expressions has real roots and therefore only one of the boundary currents can have such a control. In physical terms the explanation for this is rather simple. If the change in barotropic velocity due to the shear effect and mean flow effect act in opposition at one wall, they must reinforce on the other wall (where the sign of the barotropic shear velocity is reversed but that of the mean barotropic velocity is the same).

The possibility of three types of controls leads to a rich variety of steady solutions and we explore a few examples. The situation is simplified by the fact that different types of controls cannot arise at different locations within a particular boundary flow unless a hydraulic jump or other dissipative features occur. We will assume that the channel contains a simple contraction as shown in Figure 5.9.1b and that the mean barotropic flow $V = Q/wz_T$ is positive. Different types of behavior can easily be illustrated using a two-step graphical approach. First, changes in w must be related to changes in strangulation $s_{\pm}(w)$ using (5.9.12). A sample of curves showing this relation for various ranges in Q/z_T and Δ appears in Figure 5.9.2. Next, s_{\pm} must be related to $\eta_{\pm}(s)$ using (5.9.11). Examples of this relation, which depends on μ_{\pm} , are shown in Figure 5.9.3.

The procedure then is to use Figure 5.9.2 curve to determine the variation of the strangulation function $s_{\pm}(w)$ along the channel, then use Figure 5.9.3 to find the corresponding solution. Each frame in the former shows two curves corresponding to the strangulation function for the right (+) and left (-) boundary layers. In the case of Frame c, the two curves coincide. A virtual control must, in view of (5.9.14) occur where $s_{\pm}(w)$

⁴ This solution has elements in common with one of the nonrotating solutions discussed in connection with the curved .50 energy contour in Figure 5.3. One of these is the lock exchange flow having $v_1 = -v_2$ at the virtual control. The other is a unidirectional flow having $v_1 = v_2$. It is this second solution which is analogous to our rotating boundary flow.

very rough draft-not for distribution

or $s_-(w)$ is zero whereas a remote control occurs where $s_+(w)$ or $s_-(w)$ has a minimum or maximum. A narrows control occurs where w itself is a minimum.

Turning to Figure 5.9.3 we see that each frame has two curves corresponding to the two solutions of the quadratic equation (5.9.11). Note that the s_{\pm} -axis in Frame c corresponds to the similarity solution. It is no longer the case that the two curves represent flow in the different boundary layers; rather each curves gives a possible solution for either boundary layer. The difference in left and right boundary layers at a particular point on a particular curve is that one solution is subcritical and the other supercritical at that point. In making these designations, we use the convention that supercritical (subcritical) flow allows wave propagation in the same (opposite) direction as the mean barotropic velocity V , here assumed to be positive. In particular, use of the definition of s_{\pm} in (5.9.9) leads to

$$c_{\pm} = \pm(\hat{\delta}^{1/2} - 1)(\eta_{\pm} + \frac{1}{2}s_{\pm}),$$

and therefore

$$c_+ = (\hat{\delta}^{1/2} - 1)(\eta_+ + \frac{1}{2}s_+) \quad \begin{array}{l} >0 \text{ (supercritical)} \\ =0 \text{ (critical)} \\ <0 \text{ (subcritical)} \end{array}$$

for the right-hand boundary layer, and

$$c_- = -(\hat{\delta}^{1/2} - 1)(\eta_- + \frac{1}{2}s_-) \quad \begin{array}{l} >0 \text{ (supercritical)} \\ =0 \text{ (critical)} \\ <0 \text{ (subcritical)} \end{array}$$

for the left-hand boundary layer.⁵ Critical flow states must therefore occur on the dashed diagonals $\eta_{\pm} = -\frac{1}{2}s_{\pm}$ in Figure 5.9.3. The flow is supercritical or subcritical above or below this diagonal depending on the sign of $(\hat{\delta}^{1/2} - 1)$ and on which boundary layer is being examined. Figure 5.9.3 has been labeled assuming that $\hat{\delta} < 1$ and thus supercritical flow for the left boundary layer lies above. The leading label on each curve applies to the left-hand boundary layer, while the labels in parenthesis apply to the right-hand boundary layer. A virtual control requires both $\eta_- = s_- = 0$ or $\eta_+ = s_+ = 0$ and these are possible only in Figure 5.9.3c. A narrows control or a remote control must occur at a minimum or maximum of the solution curve, and this is possible only in Figure 5.9.3b.

The reader who has become frustrated with the details of this narrative will benefit from exploration of a few example, which we now do. Attention is limited to the left hand boundary layer and the channel geometry is as shown in Figure 5.9.1b with entrance and exit width w_o , and minimum width w_m .

⁵ These definitions are sensible for a dynamically wide channel, since the boundary layers can be treated independently; finite channel widths would require some rethinking.

(a) A narrows control

Suppose that $\Delta > 1$ so that the relation between w and s_{\pm} is given by Figure 5.9.2a. The lower curve applies to the left boundary layer. As one moves from the mouth of the channel ($w=w_o$) to the narrowest section ($w=w_m$), s_{\pm} decreases from values s_1 to s_2 and increases back to s_1 , as indicated. To find the corresponding solution, one must apply the variation in s_{\pm} to the relevant frame and curve in Figure 5.9.3. The choice depends on the value of μ_{\pm} . Since we are interested in the left wall boundary layer, we focus on μ_{-} and choose a value < 0 (Figure 5.9.3a). There are two possible solutions corresponding to the two curves. Choosing the left-hand curve gives a supercritical solution while choosing the right-hand curves gives a subcritical solution. Either curve gives a legitimate solution over the established range of s_{\pm} . In either case the flow remains supercritical or subcritical through the contraction and there is no control.

If we instead choose $\mu_{-} > 0$, then the solution shifts to the curves of Figure 5.9.3b and a control is possible. Beginning at $s_{\pm}=s_1$, which is > 0 for our example, one must first select a solution branch of the left hand curve. Choosing the subcritical branch places the solution at $\eta_{\pm}=\eta_3$ as indicated on the plot. Lowering s_{\pm} from this value causes η_{\pm} to increase. A sufficient increase places the solution at the minimum ($\eta_{\pm}=\eta_2$) of the curve, where the flow is critical. If s_2 lies at this maximum, as shown in the figure, then the solution continues onto the supercritical branch in the usual manner and the flow downstream of the narrows ($\eta_{\pm}=\eta_1$) is supercritical. The solution just described contains a narrows control. It can be shown that continuation from the subcritical branch to the supercritical branch (rather than back along the subcritical branch) is the only choice that gives a smooth solution, a matter explored in Exercise 4.

(b) A remote control.

Next suppose that $\Delta < 1$, so that the strangulation function $s(w)$ is given by the lower curve of Figure 5.9.2d. Suppose further that w lies in the indicated range $w_o \leq w \leq w_m$ such that s_{\pm} reaches its maximum value for an intermediate w , as indicated. As one moves into the channel, the value of s_{\pm} increases then decreases before the narrowest section is reached. Downstream of the narrowest section, s_{\pm} increases back to its maximum value and then decreases. Switching now to Figure 5.9.2, we again choose $\mu_{\pm} > 0$ (frame b) and note that the solution now lies along the lower, right-hand curve. We attempt to trace a solution beginning along the subcritical branch at $s_{\pm}=s_1$. Moving from the entrance into the channel causes s_{\pm} to increase and to reach its peak value s_m before the narrows is actually reached. We have arranged this point to coincide with the maximum of the solution curve. If one continues past this remote control, s_{\pm} retreats to lower values as the channel narrows but solution moves onto the supercritical branch. When the narrowest section ($w=w_m, s_{\pm}=s_2$) is reached, the flow is supercritical. Downstream of this point the above sequence is rewound. As the channel widens, the flow passes back through a second remote control and returns to a subcritical state. Note that the flow at this second control section is subject to the same instability discussed in connection with

single layer flows; wave propagation is locally towards the critical section from upstream and downstream. We thus anticipate that a hydraulic jump or other dissipative feature may occur there.

(c) A virtual control

Virtual control implies $s_- = 0$ and therefore is possible only for strangulation curves which cross the w -axis in Figure 5.9.2. Suppose that $\Delta > 1$, so that the lower curve of Figure 5.9.2 applies if the range of w is such that s_- has a zero crossing. In this case, s_- will be positive at the entrance and exit of the channel, but negative at the narrowest section. Now this range of s_- to Figure 5.9.3c, which shows the solutions with possible virtual controls. At the channel entrance, $s_- > 0$ and a choice of subcritical there forces one to select diagonal curve. As the width narrows, the solution passes through a virtual control at the origin, and continues onto the supercritical branch until the narrowest section is reached. This sequence is retraced as the narrows is passed, with the proviso that instability may occur at the downstream virtual control. The solution therefore behaves in a similar way to that with a remote control, as just described. The similarity solution, which is represented by the s_- axis in Figure 5.9.3, is supercritical at the upstream entrance in this case.

Where the diagonal solution passes through the origin of Figure 5.9.3c, it is conceivable that it could jump from the diagonal curve onto the similarity solution, or *vice-versa*. As explored in Exercise 5, such a jump would generally involve a discontinuity in $\partial \eta_- / \partial y$ or $\partial^2 \eta_- / \partial y^2$ at the control, and can therefore be ruled out.

These examples show only some of the possible behavior that is consistent with the model. One can invent a variety of solutions by matching different Figure 5.9.2 forcing curves with different Figure 5.9.3 solutions curves. No known attempts have been made to verify any of these solutions. The main purpose has been to demonstrate the physical mechanism associated with the forcing of a boundary current by a larger scale flow and the novel features that can arise when that external flow is sheared.

Exercises

- 1) Obtain the expression (5.9.5) for the total volume flux.
- 2) Derive the expression for the internal Kelvin wave speeds (5.9.8) in the wide-channel limit and with attached interfaces. (You can work through the full nonlinear version of the calculation by first noting that the expressions for velocity and layer depths derived above remain valid when the flow is time-dependent. The characteristic form of the equations governing on a certain sidewall may be obtained by evaluating the layer momentum equations there and substituting the expressions for v_n and d_n that follow from the profiles.)

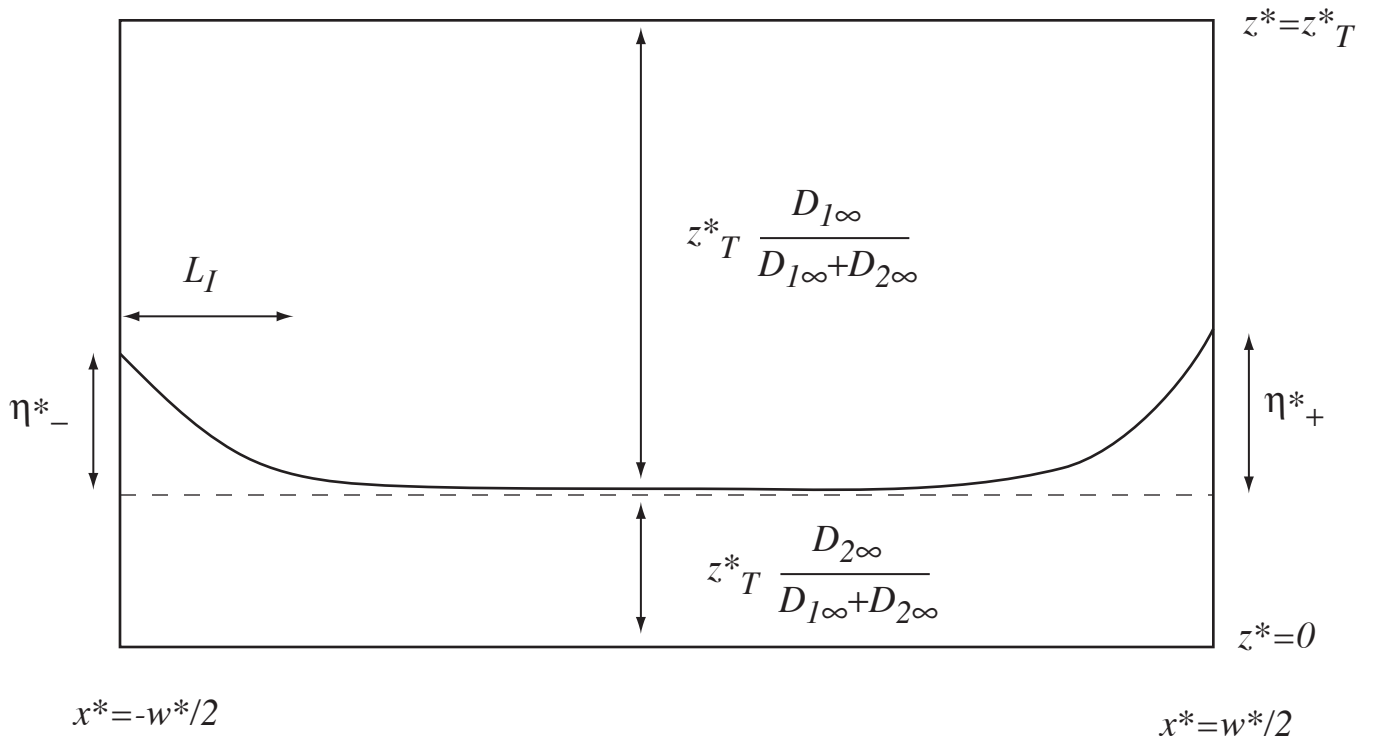
- 3) We noted that (5.9.14) implies separation of the critical flow from the channel side walls when $\hat{\delta} = 1$. An exception occurs when the numerator of the right hand side of this equation vanishes. Explore this case and describe the flow that results.
- 4) For a narrows control show that continuation from the upstream subcritical branch to the downstream subcritical branch of the lower left solution curve in Figure 5.9.4c is the only choice that avoids singularity.
- 5) At a virtual control, show that the solution cannot jump from the similarity solution $\eta_- \equiv 0$ to the solution $\eta_- = -s_-(y)$, or *vice-versa*, without incurring a discontinuity in $\partial\eta_- / \partial y$ or $\partial^2\eta_- / \partial y^2$ unless virtual, remote, and narrows controls coincide at the narrowest section.

Figure Captions

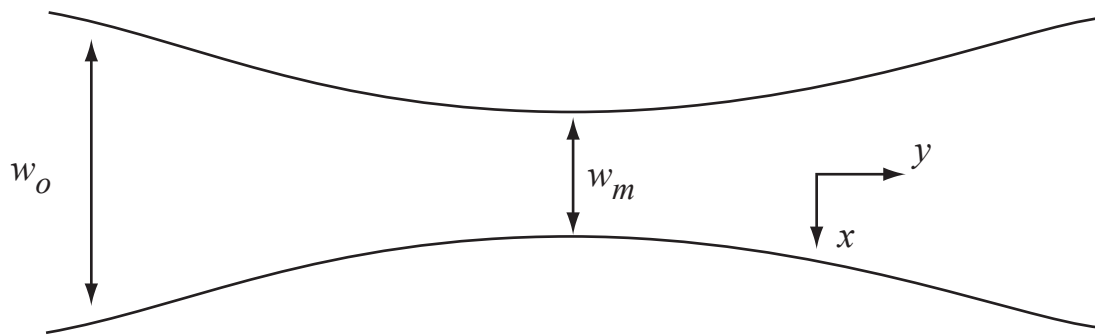
Figure 5.9.1 Definition sketches for two-layer flow in a wide channel with a horizontal bottom.

Figure 5.9.2 The strangulation parameter s_{\pm} as a function of width w according to equation (5.9.12). The general geometry of the curves of s_+ and s_- takes four different forms according to the value of Δ relative to unity, and to whether Q is finite. These four forms are illustrated by (a-d). The numerical values used to obtain the plots are (a) $\Delta=5$, $Q/z_1=1$; (b) $\Delta=1$, $Q/z_1=1$; (c) $\Delta=5$, $Q/z_1=0$; (d) $\Delta=0.5$, $Q/z_1=2$

Figure 5.9.3 The relationship between η_{\pm} and s_{\pm} according to (5.9.11). Frames (a)-(c) give the general geometry of the solution curves for $\mu_{\pm} < 0$, $\mu_{\pm} > 0$, and $\mu_{\pm} = 0$. Each solid curves in each frame may represent potential solution for either boundary layer. In (c) the s_{\pm} -axis is a solution curve. The operational difference between left and right boundary layers is contained in the subcritical or supercritical designation on each curve. Here the labels have been chosen assuming that $\hat{\delta} < 1$. The leading label on each curve then corresponds to the left-hand boundary layer while the label in parenthesis corresponds to the right-hand layer. When $\hat{\delta} > 1$ this order is reversed. The dashed diagonal curve in each frame indicates the possible locations of critical flow. The numerical values of μ used to make frames (a), (b), and (c) are 1,-1, and 0. The quantities Δ and $-\Delta / \hat{\delta}$ marked in (a) indicate limits outside of which the flow becomes separated from one of the sidewalls. These limits are given without assigned value and apply in all three frames.



(a)



(b)

Figure 5.9.1

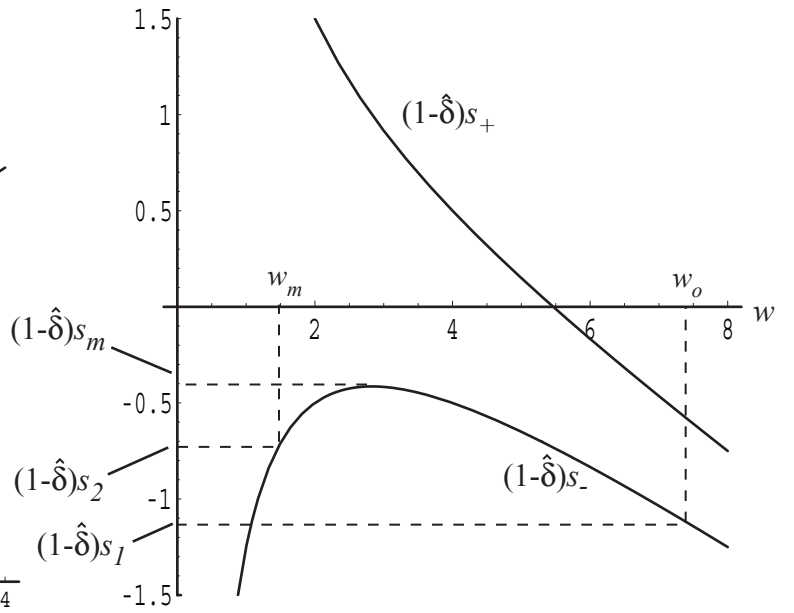
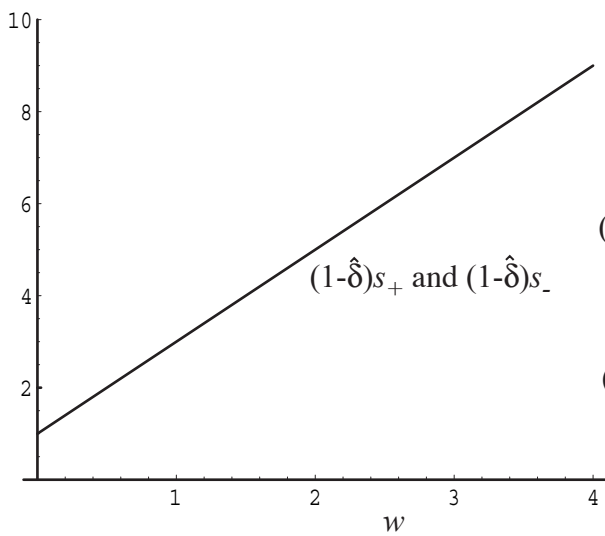
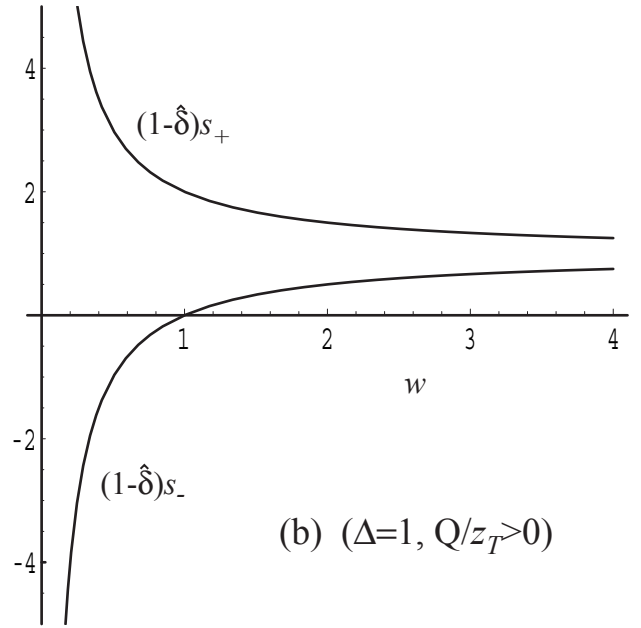
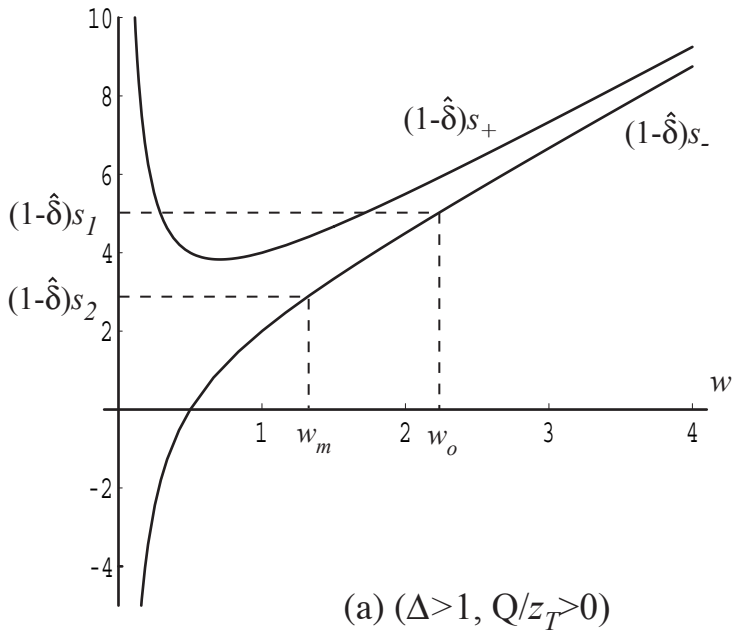


Figure 5.9.2

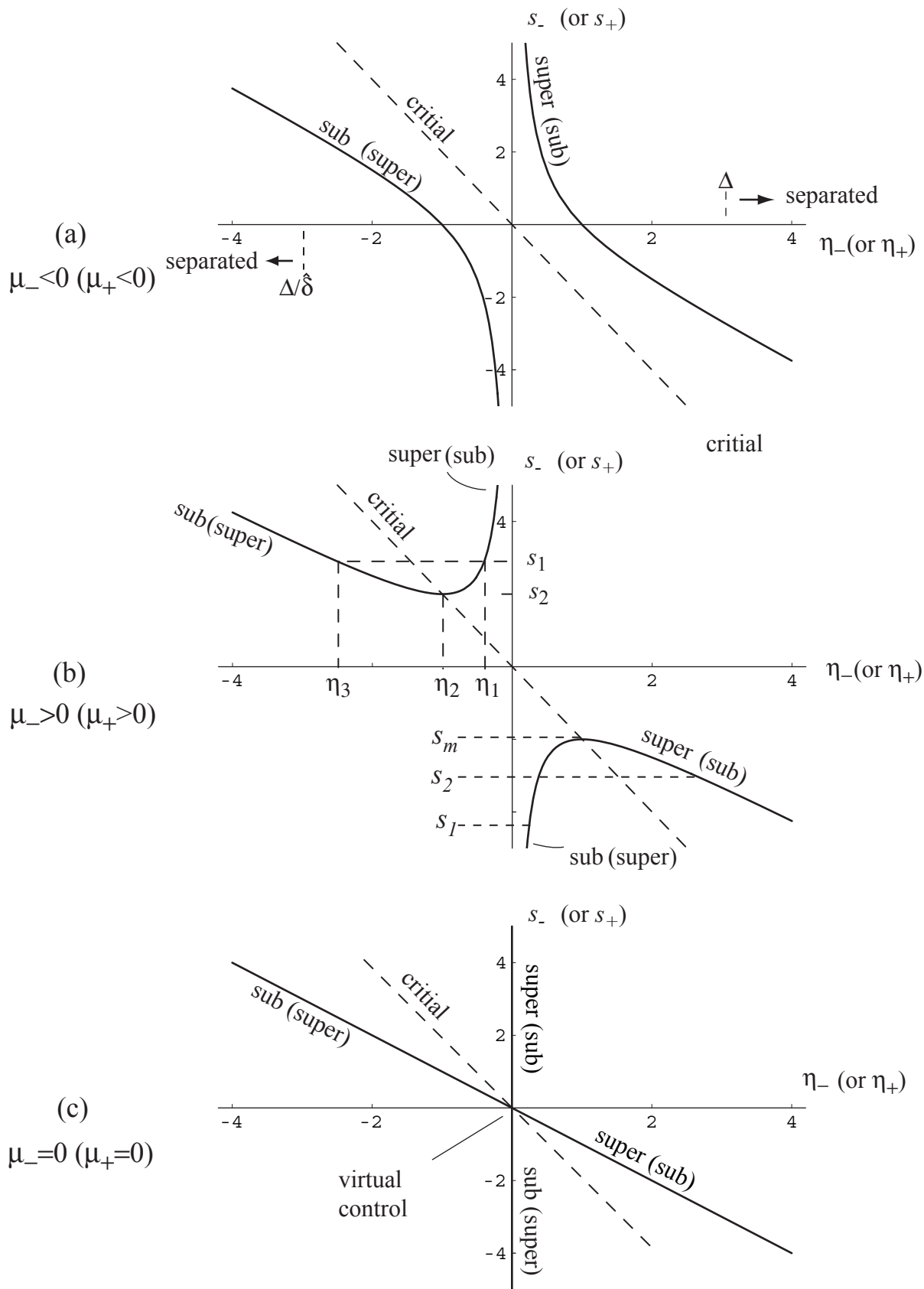


Figure 5.9.3